Retinal Blood Vessel Extraction Using a New Enhancement

by Bambang Suprihatin

World Scientific
www.worldscientific.com

Retinal Blood Vessel Extraction Using a New Enhancement Technique of Modified Convolution Filters and Sauvola Thresholding

Erwin*

*Department of Computer Engineering
University of Sriwijaya
Jalan Raya Palembang-Unsri KM 32 Indralaya
South of Sumatera, Indonesia
erwin@unsri.ac.id*

Hadrians Kesuma Putra

*Department of Medical, University of Sriwijaya
Jalan Raya Palembang-Unsri KM 32 Indralaya
South of Sumatera, Indonesia
hadrianskesuma@fk.unsri.ac.id*

Bambang Suprihatin

*Department of Mathematics
University of Sriwijaya
Jalan Raya Palembang-Unsri KM 32 Indralaya
South of Sumatera, Indonesia
bambangs@unsri.ac.id*

Fathoni

*Department of Information System
University of Sriwijaya
Jalan Raya Palembang-Unsri KM 32 Indralaya
South of Sumatera, Indonesia
fathoni@unsri.ac.id*

The retinal blood vessels in humans are major components with different shapes and sizes. The extraction of the blood vessels from the retina is an important step to identify the type or nature of the pattern of the diseases in the retina. Furthermore, the retinal blood vessel was also used for diagnosis, detection, and classification. The most recent solution in this topic is to enable retinal image improvement or enhancement by a convolution filter and Sauvola threshold. In image enhancement, gamma correction is applied before filtering the retinal fundus. After that,

---

*Corresponding author.

the image should be transformed to a gray channel to enhance pictorial clarity using contrast-limited histogram equalization. For filter, this paper combines two convolution filters, namely sharpen and smooth filters. The Sauvola threshold, the morphology, and the medium filter are applied to extract blood vessels from the retinal image. This paper uses DRIVE and STARE datasets. The accuracies of the proposed method are 95.37% for DRIVE with a runtime of 1.77 s and 95.17% for STARE with 2.05 s runtime. Based on the result, it concludes that the proposed method is good enough to achieve average calculation parameters of a low time quality, quick, and significant.

Keywords: Blood vessels; image processing; retinal; Sauvola threshold; segmentation.

1. Introduction

The retinal vessels have a major contribution to the diagnosis of retinal diseases. Retinal blood vessel recognition is a major step in detecting retinal fundus disease, shape, and size. The retinal image consists of the retinal nervous system, fluid, and vessels. The design of the blood vessels in the retinal image is formed from lines so that disruption of the retinal blood vessels becomes a serious problem.[1] Thus, blood vessels are the primary medical object for eye syndrome.[2]

The main step in detecting eye disease is the removal of the retinal blood vessels.[3] Digital retinal fundus removal is an important phase in many computerized pathological procedures, such as diabetic retinopathy, macular degeneration, glaucoma, and retinal artery occlusion.[4] In high-resolution retinal images, ophthalmologists can diagnose disease by extracting blood vessels, optic disc, and macula.[5] Problems that often arise are due to poor quality retinal images in blood vessel removal. Previously, the retinal vein extraction technique had its level of difficulty. Vessel recognition can be characterized by color, shape, gradient, contrast, and so on. However, many features do not meet the diagnostic requirements.

The previous research studies in recent years have concentrated on methods that have their properties. Dash[6] proposed the three-phase process segmentation approach where the first step of image processing was CLAHE. The segmentation used the ISODATA. In the final phase, morphological washing was carried out to decrease the noise caused during the segments. Nevertheless, the result is not accurate depending on the ground truth dataset and halted at ISODATA which has a certain digit significance when the maximum value was found in the batch amount.

Dash and Bhoi[7] suggest an uncontrolled vascular retinal extraction approach. The segmentation method uses three stages, namely pre-processing, removal, and post-processing. The segmentation contains machine learning systems but uncontrolled systems and pre-processes are not described. Only gamma correction is needed to improve the result of segmentation parameters. Biran *et al.*[3] worked only in the form of images of blood vessels, but at the bottom of the blood vessels, there were still unnecessary dots. Guu *et al.*[8] proposed an automated retinal vessel extraction technique and classified it into three levels of monitoring and screening categories. This method does not operate very much and is very sensitive to noise. This technique also shows that misclassified pixels present images of retinal vessels.

According to Soomro *et al.*,[9] the CLAHE method provides a clearer image, but the vascular test decreases due to failure of detection of small vessels. Several processes discussed in the experiment can identify diabetes in the retina of the eye. Abdallah *et al.*[10] used a multiscale medial technique which showed that the suggested technique worked well, but the retinal fundus was so small that it was considered a canal.

Kamble *et al.*[11] changed the extension phase and used many techniques involving interference. This technique causes a slight increase in retinal vascular thickness after post-processing. Khomri *et al.*[12] used an elite bee colony-guided multi-objective technique (EMOABC) experiment as a preprocessed segmentation phase with a top cap and blue canal, while retinal vessels remained less precise. They use large system requirements so that for comparison with previous studies the accuracy is still small.

In the description, the author noted various methods in the segmentation of retinal blood vessels. It was performed for medical purposes. We used therefore the segmentation of the threshold of the retina vessels and the enhanced image of the retina fundus filter.[13–17]

The blood vessels are segmented using the Maximum Principal Curvature algorithm. Before the segmentation process, images are filtered using Gaussian filters, and the optic disc removal is performed. After that, the segmentation of vessels uses Wolf thresholding to convert images into binary images.[13] Poor quality images will be corrected and performed with a median filter removal filter. In the pre-processing stage, two contrast methods are used, namely contrast stretching histogram equalization and CLAHE. Increase the contrast by stretching the existing value in the image at a certain intensity. Contrast stretching will stretch, increase, and decrease the contrast of the image. The median filter is a filter for image enhancement that will filter out noise.[14] But, some images such as medical ultrasound images are mainly degraded by an intrinsic noise called speckle. Therefore, de-speckling is a main pre-processing stage for degraded images.[18,19]

The segmentation process uses multilevel thresholding with the Otsu function. The method used is to combine Otsu multilevel thresholding with morphological operations.[15] In addition, multilevel thresholding segmentation is combined with the convolutional neural network. Multilevel thresholding produces disease characteristics by segmenting blood vessel morphology accurately. The enhancement process is carried out automatically with a Gaussian filter and Sobel edge detection to detect blood vessels.[17] Next, we conducted experiments to develop retinal blood vessel segmentation using dynamic threshold and image enhancement filters. The enhancement process uses the latest approach, namely the Butterworth Bandpass filter. Butterworth bandpass filter is used as the smoothing and sharpening image.[16]

This research uses the most advanced image filters in the pre-processing stage. Retinal blood vessel binary image repair produces smooth images with CLAHE. After the grayscale was obtained, morphology was performed to improve the image of the damaged retinal blood vessels. Then, a median filter is used to reduce noise and

remove unnecessary pixels. After that, the vessels were segmented using the Sauvola threshold method. This stage is expected to obtain the desired results.

The approach in this paper has a novelty, namely the image enhancement filter system which is a combination of two convolution filters, namely sharpen filter and smooth filter. The image enhancement filter had the role of making a range of pixel values in the retinal image so that the pixel values had a homogeneous significant difference between the histogram system of blood vessel pixels and non-pixel retinal vessels. As a result, the image enhancement filter had a very good impact to fulfill as a pre-process requirement for the Sauvola threshold with pixel-based processes.

In this paper, a significant contribution is made to image enhancement filters which were very valuable in adapting the pixels forming the binary with the Sauvola threshold method, the measuring parameters value, and the execution time significantly was more than in previous studies.

2. Materials and Method

In this paper, the Sauvola threshold and the retina fundus image improvement filter are used. The retinal fundus is divided into the Sauvola threshold. This enhances the correction of a game and CLAHE image by removing poor-quality retinal blood vessels and then an image filter to sharpen the image, making it smooth. After treatment, some non-pixel vessels such as small pixels are removed using remove small pixels, median filters, and morphological closing. The stages of the proposed method for the segmentation of the blood vessels are illustrated in Fig. 1.

2.1. *Pre-Process*

The first stage is to produce an image of the retina fundus as an input image. Fundus retina images receive information from the datasets DRIVE and STARE. The information in the input image phase is received. The pre-processing is then performed to improve image precision, processing, color shift, etc. Several techniques are performed in pre-processing as follows:

2.1.1. *Gamma Correction*

In the first phase, the image entry is converted into gray using the Gamma correction procedure to enhance the luminosity of the image. Make the region in the blood vessels recognizable more clearly in comparison with the image's situation in the patient.[17] The equation used for gamma correction[7,20] is in Eq. (1).

$$L_{\text{out}} = CL_{\text{in}}^{\gamma}, \tag{1}$$

where $L_{\text{out}} = $ output of luminosity, $C = $ constant, $\gamma = a$ gamma value and $L_{\text{in}} = $ input of luminosity.

Transformations can be designed to approximate a certain gamma with a linear portion near zero to avoid having an infinite slope $K = 0$, which can cause numerical problems. The continuity condition for the curve C_{linear} gives the linear domain
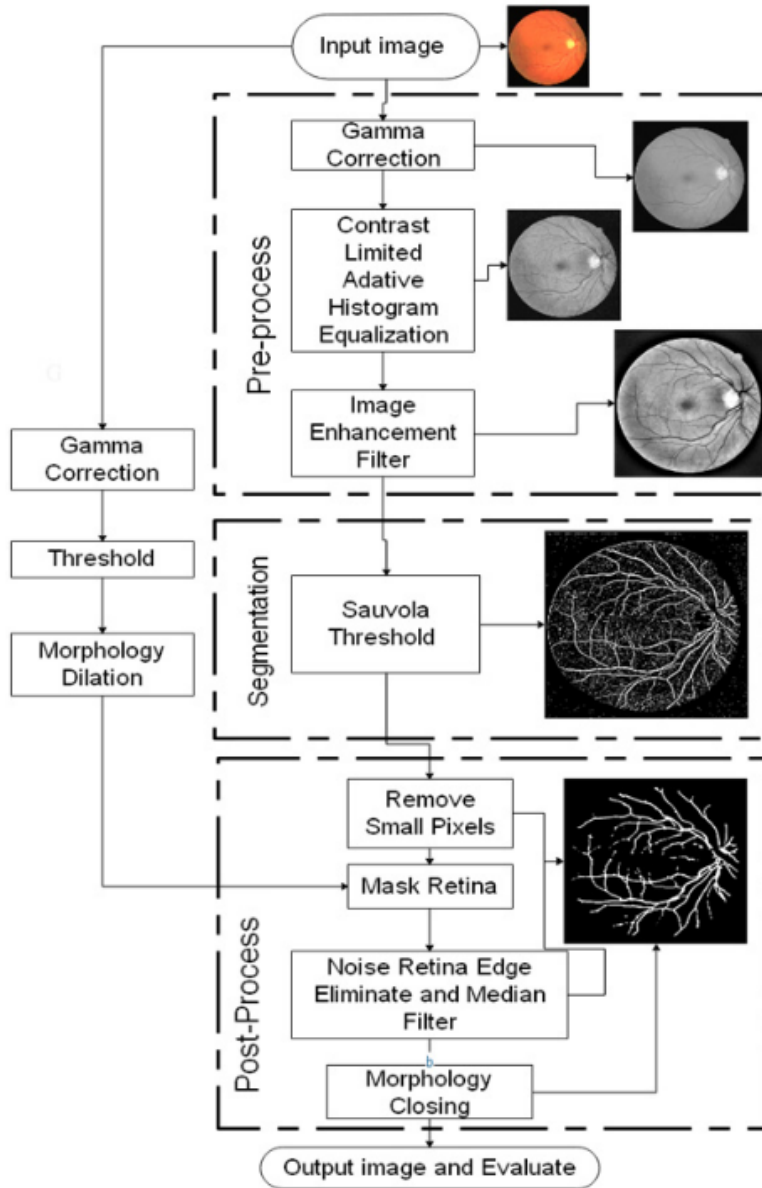
Fig. 1. Proposed method block diagram. The block with dashed lines shows the new techniques proposed in the pre-processing, segmentation, and post-processing stages.

threshold β

$$\left(\frac{K_0 + a}{1 + a}\right)^{\gamma} = \left(\frac{K_0 + \alpha - 1}{\alpha}\right)^{\gamma} = \frac{K_0}{\emptyset} := \beta.$$

Solving for $K = 0$ gives two solutions which are usually rounded. However, for the slopes, they match as well; then, we must have

$$\gamma\left(\frac{K_0 + a}{1 + a}\right)^{\gamma - 1}\left(\frac{1}{1 + a}\right) = \gamma\left(\frac{K_0 + \alpha - 1}{\alpha}\right)^{\gamma - 1}\left(\frac{1}{\alpha}\right) = \frac{1}{\emptyset}.$$

If the two unknowns are taken to be K_0 and $\emptyset$, then we can solve to give

$$K_0 = \frac{a}{\gamma - 1} = \frac{\alpha - 1}{\gamma - 1}$$

$$\emptyset = \frac{(1+a)^{\gamma}(\gamma-1)^{\gamma-1}}{(a^{\gamma-1})(\gamma^{\gamma})} = \frac{\alpha^{\gamma}(\gamma-1)^{\gamma-1}}{((\alpha-1)^{\gamma-1})(\gamma^{\gamma})}.$$

The concept of gamma can be applied to any nonlinear relationship. For the power law relationship, $L_{\text{out}} = C\,L_{\text{in}}^{\gamma}$, the curve on a log–log plot is a straight line, with slope everywhere equal to gamma (slope is represented here by the derivative operator):

$$\gamma = \frac{d\log(L_{\text{out}})}{d\log(L_{\text{in}})}.$$

Gamma correction has a setting in entering the brightness intensity parameter of the grayscale image which is called the gamma value. The gamma value provides variations in the brightness of the image. This variation has a strong enough impact on retinal blood vessels, both of which will dim, disappear, and be visible when continued in the next process. Gamma correction is very important in adjusting the contrast to get the focus to the retinal blood vessels by getting the desired intensity so that it has a good impact on the CLAHE process. The corrected images may appear either bleached or too dark as needed; however, in this study, the gamma value of 0.9 was used as the standard. The greater the gamma value for grayscale correction, the darker the image will be and the brighter it will be as it approaches the 0 gamma value.

The following is the source code used for Gamma correction steps:

```
gray = cv2.cvtColor(img, cv2.COLOR_BGR2GRAY)
gamma= np.array(255*(gray/255)**0.9,dtype='uint8')
img3 = cv2.hconcat([ gamma] )
cv2.imshow('gamma',img3)
```

2.1.2. *Contrast-Limited Adaptive Histogram Equalization*

The adjustable histogram equalization (CLAHE) is used. CLAHE aims to enhance image performance by small comparison.[21] This is very helpful to clarify the item adopted with the histogram stage from the gray region and the fluid vessel and others on each pixel in the same way.[7] Contrast enhancement at this stage becomes very important in making that much difference in the range of histogram grayscale image to pixels of blood vessels and pixels instead of blood vessels.

CLAHE is useful for improving the quality of low-contrast images. This is very useful for Gamma correction results, which can further clarify the object taken with the histogram level in a few gray range areas and the blood vessels, and other parts are evenly distributed in the pixels that make up each block. This study uses 2 (two) parameters, namely cliplimit and tileGridSize. The number of cliplimits in CLAHE is

useful for limiting the contrast of the image while the tileGridSize size for optimal mapping depends on the input image. As a result of CLAHE, the retinal blood vessels' area is dark in color, while apart from the retinal blood vessels, it is gray and looks bright.

This step is done by increasing each pixel in the retinal image that has low contrast. Below is the source code for increasing image contrast using the CLAHE method.

```python
from scipy import ndimage, misc
import imageio
import numpy as np
import os
import cv2
def main():
    outPath = "clahe/"
    path = "RGB/Green"
    for image_path in os.listdir(path):
        input_path = cv2.imread(path + image_path)
        clahe = cv2.createCLAHE(clipLimit = 2.0,
tileGridSize=(8,8))
        final_img = clahe.apply(input_path,0)
        cv2.imwrite('clahe/clahe_' + image_path + '.jpg',
final_img)
if __name__ == '__main__':
    main()
```

In the source code, cv2.imread is used to read the input image to be contrasted and then stored in the input_path variable. cv2.createCLAHE is a function that is used to improve the image quality of the green color channel separation that still has low contrast so that it can be seen. Parameters used include cliplimit and title-gridsize. The cliplimit parameter is used to determine the contrast enhancement limit of the input image, while the titlegridsize parameter is used to determine the size of the number of grids to perform histogram equations. Then, cv2.imwrite is used to save the contrast enhancement result of the input image.

2.1.3. *Combined Enhancement Filtering*

The next process performs an image enhancement filter process that functions to increase the retinal image from the CLAHE process so that a smooth image is obtained using a 3×3 kernel on the average filter and sharpens the image. There are two processes at this stage, namely sharpen and smoothing, using the kernel filtering techniques. The sharp image functions as the strength of the item in the pixel layout becomes thicker while the smoothing filter is the method used to stretch undesired items due to the almost identical size of the grayscale. This is the last stage of the

pre-processing in the imaging improvement filter process, which has an important role to play in getting blood vessels from the retina. With the equation for sharpening image and average filter (smoothing filter) in Eq. (2), followed by the kernel sharpen filter in Eq. (3) and smoothing filter in Eq. (4), the following is obtained.

$$h(x,y) = f(x,y) * g(x,y)$$
$$= \sum_{a=-\infty}^{\infty} \sum_{a=-\infty}^{\infty} f(a,b).g(x-a,y-b), \tag{2}$$

$$f(x,y) = \begin{bmatrix} 0 & -1 & 0 \\ -1 & 5 & -1 \\ 0 & -1 & 0 \end{bmatrix}, \tag{3}$$

$$g(x,y) = \frac{1}{25} \begin{bmatrix} 1 & 1 & 1 & 1 & 1 \\ 1 & 1 & 1 & 1 & 1 \\ 1 & 1 & 1 & 1 & 1 \\ 1 & 1 & 1 & 1 & 1 \\ 1 & 1 & 1 & 1 & 1 \end{bmatrix}, \tag{4}$$

where $h(x, y)$ is a filter for image enhanced $f(x, y)$, that is, the kernel filter, and $g(x,y)$ are the inputs of images.

The syntax for the image enhancement filter stage is as follows:

```
kernel_sharpening = np.array([[ 0,-1,0],
                             [-1, 5,-1],
                             [ 0,-1,0]])
sharp=cv2.filter2D(cl1, -1, kernel_sharpening)
cv2.imshow('sharpen', sharp)
kernel = np.ones((2,2),np.float64)/25
average = cv2.filter2D(sharp,-1,kernel)
cv2.imshow('sharpen+smooth', average)
```

2.2. *Retinal Fundus Segmentation*

The next step is to extract the retinal image to get the vessels of the retinal blood after the preparation process. It uses the Sauvola threshold at this stage. Sauvola threshold is a local threshold method that can improve threshold calculations with a range of dynamic values from the standard gray-scale image deviation value.[22,23] In this stage, the process is done in stages with pixels one by one and supported by neighboring pixels. The equation for the Sauvola threshold is as follows:

$$L(x,y) = \begin{cases} 1, & \text{if } I_E(x,y) > m(x,y) * \left(1+k*\left(\frac{s(x,y)}{R}-1\right)\right) \\ 0, & \text{if } I_E(x,y) \leq m(x,y) * \left(1+k*\left(\frac{s(x,y)}{R}-1\right)\right) \end{cases}, \tag{5}$$

where W is the processed block, Nw is the number for each block W, C is the constant and L is the threshold (x, y).

Segmentation for Sauvola threshold is done with the following source code:

```
threshold_sauvola = skimage.filters.threshold_sauvola
(average, window_size=11, k=0.17)
binary_threshold_sauvola = average > threshold_sauvola
indices = binary_threshold_sauvola.astype(np.uint8)
indices*=255
inverse = cv2.bitwise_not(indices)
cv2.imshow('sauvola thres',inverse)
```

2.3. *Post-Process*

The final step is the post-process consists of cleaning small pixels, median filter, making retina mask, and morphology. There are small annoying pixels or noise adjacent or far away from the pixel of the blood vessel. Therefore, it is not necessary to clean tiny pixels. When small pixels are deleted, the binary images still have a retinal edge, which is regarded as noise. This can, therefore, be removed by first using the retina image mask. The steps of making retinal prints, separating images, and performing morphology by taking the initial image and making unique resonance adjustments will achieve successful retinal test results.

2.3.1. *Elimination of noise edge retina and median filter*

After the removal image of small pixels and the formation result of the retinal mask have been taken, removal is then carried out between the removal results of small pixels and the retinal mask formation result. The results are in the form of binary images without edge noise, although further enhancements are required to the blood vessels that are still close together with small pixels. In that portion of the method, therefore, the median filter function is played. The median filter is a nonlinear method for digital filters that often is used to remove images or pulses from the noise. The equation for medium filters[24] is as follows:

$$y[m, n] = \text{median}\{x[i, j]\}, (i, j)\epsilon\,\omega, \tag{6}$$

where ω represents a user-defined environment, centered around the location $[m, n]$ in the image.

The median filter works by evaluating the brightness level of a pixel and determining which pixel increases its brightness. Below is the source code used in the image cleaning stage from noise using a median filter.

```
import cv2
#input image
img=cv2.imread("clahe_im0002.jpg")
#median filtering
```

```
image_median = cv2.medianBlur(img,3)
#saving median filter result
cv2.imwrite('median_filter/median_im0002.jpg',image_median)
cv2.waitKey(0)
cv2.destroyAllWindows()
```

In the source code, cv2.imread is used to read the input image data. Then cv2.medianblur() is used to take the median value of all pixels under the kernel area and the center element and replace it with the median value that has been obtained. In the source code, 30% noise is added to the original image. Then, cv2.imwrite is used to save the image cleaning results from noise into the median_filter folder.

2.3.2. *Morphology closing*

Following the retinal border noise and a median filter elimination, blood vessels will be cleared. To achieve peak assessment outcomes and performance, morphology closing is of major importance. The equation used for morphology closing is as follows:

$$A.B = (A \oplus B) \ominus B, \tag{7}$$

where A is the input image and B is the kernel for morphology closing.

3. Result

In this study, Anaconda Spyder Python 3.7 was used with device specifications, Celeron processor 2957U 1.4 GHz laptop, and Intel HD graphics 2 GB RAM. Data retinal fundus obtained from DRIVE[25] is verified and estimated at the public availability for the fundus process of this paper and STARE[26,27] dataset and results of the segmentation by PNG. One of the most widely utilized datasets for segments of retinal blood vessels is the DRIVE dataset. The image collection was split into learning and testing images. The DRIVE repository for this research's segmentation method is in TIF format. Like DRIVE, STARE was funded by the United States, National Health Institutes. Over 30 individuals participated in the venture throughout its past, with roots in dentistry, mathematics, and technology. STARE is accessible in 400 collections of real images, soil reality with the segmentation of the blood vessels, optical disks, and diagnostic cards. The STARE dataset about this research's segmentation method with a PPM layout is shown.

The following is an image dataset processing that can be seen in Fig. 2 subfigure (a). The image of the initial grayscale from the pre-process with the gamma grayscale correction can be seen in Fig. 2 subfigure (b). To display the image on the monitor exactly is a very important gamma correction. Fixed images might look blanched or too dark. The higher the gamma value, the lower the image. In this experiment, we used a gamma value of 0.9, which can be seen in Fig. 2 subfigure (b). Gamma values provide brightness variations in the image that can be seen in Fig. 2 subfigure (d).
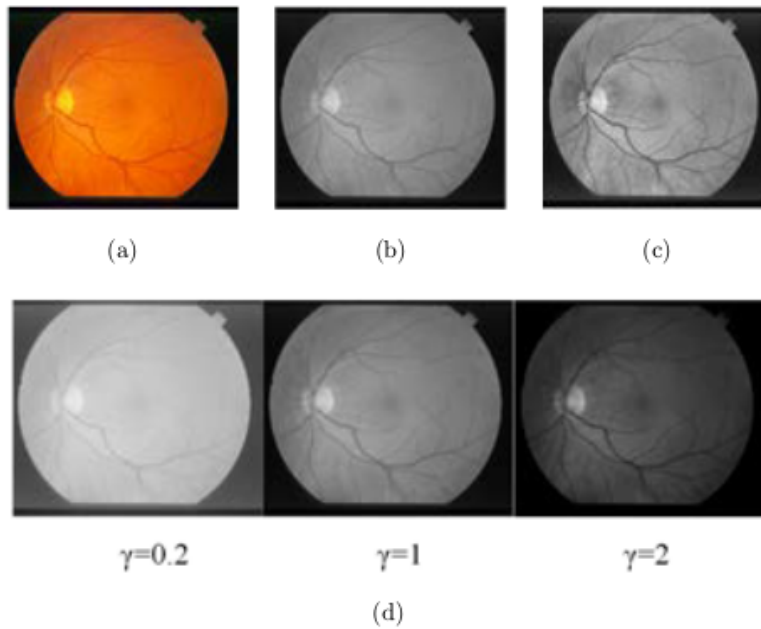
(a)   (b)   (c)

$\gamma=0.2$ $\gamma=1$ $\gamma=2$

(d)

Fig. 2. Input image and pre-processing (a) original Image,[23] (b) Gamma correction $\gamma = 1$. (c) CLAHE. (d) Gamma correction with various value Gamma ($\gamma = 0.2$, $\gamma = 1$, and $\gamma = 2$).

This variation is going to affect blood vessels strongly enough, which is either dimmed or disappeared and can be seen clearly if the next process is carried on.

Therefore, gamma correction is extremely important to adjust the contrast to blood vessels through the desired intensity to have a good effect on the CLAHE process. CLAHE makes the image contrast change sharper than the gamma correction process can be seen in Fig. 2 subfigure (c) so that the blood vessel area is dark while other than the vessels are grayscale and bright.

Gamma correction is a pre-process that is carried out for the first time with the same function as Grayscale but has a setting to enter a parameter of the brightness intensity of a grayscale image called the gamma value. Parameter_low_to_ bottom is the parameter value used for setting the low level at the bottom point while parameter_high_to_top is for setting the high level at the top point in a coordinate curve. This curve can be seen in Fig. 3.
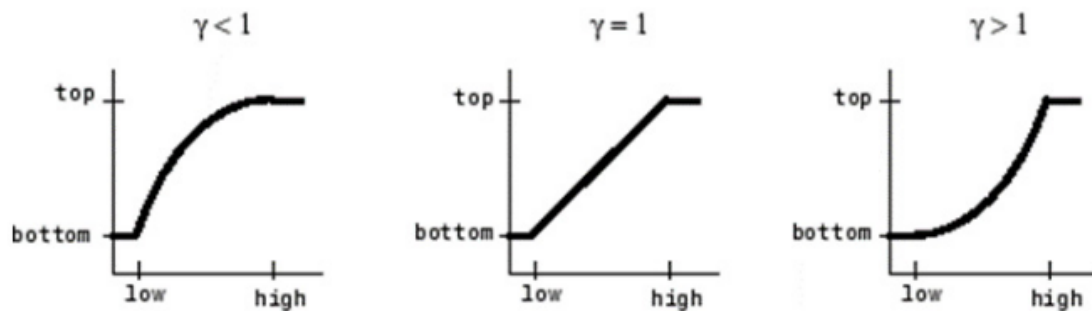
Fig. 3. A curve showing parameter_low_to_bottom parameter_high_to_top.[17]

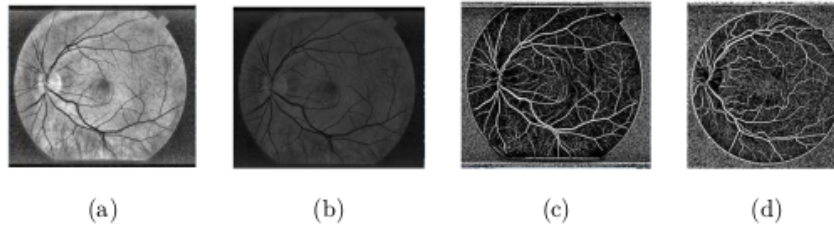|			
(a)	(b)	(c)	(d)

Fig. 4. Image enhancement filter and retina fundus segmentation. (a) sharpen image, (b) smooth filter, (c) Sauvola threshold on STARE and (d) Sauvola Threshold on DRIVE.

In Fig. 4, image enhancement filter and segmentation results for sharpen image can be seen in Fig. 4 subfigure (a) and the average filter (smoothing filter) can be seen in Fig. 4 subfigure (b). Image enhancement filter is a combination of sharpen image and the average filter (smoothing filter). Both sharpen image and average filter use filter convolution calculation techniques as can be seen in Eq. (2). In the sharpen filter process, the pixels will be changed based on the kernel in convolution with a variable arrangement of pixels which treats blood vessel pixels worth near enough binary zero in grayscale images and non-blood vessel pixels worth near binary one in a grayscale image. A significant difference in the constituent pixels of blood vessels with non-blood vessels is very useful for the next process, namely a smoothing filter. For the arrangement of the averaging pixel with the value derived from calculating the averages, the smoothing filter plays an important role. The smoothing filter will adjust the grayscale image sequence based on the pixels uniformly in the process of segmenting the retinal blood vessel area. The Sharpen image process uses a 3×3 kernel which contains a matrix ([[0, −1,0], [−1, 5, −1], [0, −1,0]]) while average filter as smoothing image use a 5×5 kernel containing a matrix 1/25 ([[1,1,1,1,1], [1,1,1,1,1], [1,1,1,1,1,], [1,1,1,1,1,], [1,1,1,1,1,]]), so that the combination of sharpening images and smoothing will have a good impact on the next process, which is the process of extracting the retina to get the blood vessels of the retina. After that, we use the Sauvola threshold which functions to make certain parts brighter while the other parts become darker or change the image to binary for STARE as can be seen in Fig. 4 subfigure (c) and for DRIVE can be seen in Fig. 4 subfigure (d). The impact of retinal blood vessel colors is darker; thus, the thresholding method is noticeable more at a root edge. Therefore, gamma correction, CLAHE, and image enhancement filter are very essential in the form, volume, and duration of the blood vessel retina. The impact varies on the image-enhancing filter method. Background removals must be made after the process, which is not necessary.

Concentration on the retinal vessels implies the retinal vessels are removed from the other hand. Removing small pixel imagery helps strip any connected components from binary images or thresholds. This has also a threshold dependence and the main CLAHE and Butterworth Gamma correction filters. Like drying of tiny points, the function of the removed small pixel is very essential too so that the medium filter can remove noise by modifying the center pixel size.
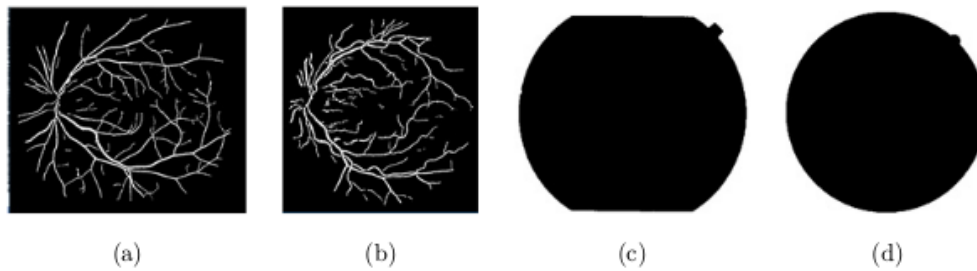
Fig. 5. Removing the background and connected small pixels on post-process (a) STARE, (b) DRIVE, (c) Retina Mask at STARE, and (d) Retina mask at DRIVE.

In the process of removing small pixels, there are still outlines on the retina, where the binary image is considered to have noise. Therefore, to eliminate noise by forming a retinal image mask, morphological dilation is carried out to get good retinal mask results.

The illustration can be seen in Fig. 5 for removing the background and connected small pixels assisted by the shape of the retina for STARE result can be seen in Fig. 5 subfigure (c) and for DRIVE result can be seen in Fig. 5 subfigure (d). The shape of the retina and mask in Fig. 5 is to minimize the result by using a mask retina to obtain a retinal mask using gamma correction, threshold, and dilation morphology with influential supporting coefficients to produce the outcome of STARE can be seen in Fig. 5 subfigure (a) and for DRIVE result can be seen in Fig. 5 subfigure (b).

Results of DRIVE and STARE image processing are shown in Tables 1 and 2. In this situation, we shall compare the DRIVE and STARE datasets with the ground truth. If the blood vessels function in line with the dataset beginning from the start of the retinal blood vessel until the finish, the assessment parameter range will be big. After repairing the image with Gamma Correction and CLAHE, an image enhancement filter is performed. This stage has 2 (two) processes, namely image sharpening and image smoothing using the convolution filter technique. The function of image sharpening is to make the intensity of the desired object denser in its pixel arrangement, while image smoothing is a technique to stretch out unwanted objects so that the grayscale range becomes almost the same. The quality of the binary image resulting from the segmentation of blood vessels is measured by calculating the peak signal noise to ratio (PSNR) value. PSNR value is good in quality if the value is more than 30 dB. The calculated PSNR values for the STARE and DRIVE datasets are 61.43 dB and 61.46 dB, respectively.

This segmentation process changes the binary image using the "cv2.normalize" syntax and compares it with the ground truth image. Next, save the processing results using the "cv2.imwrite" syntax and to close the currently running form, use "waitKey" and "destroyAllWindows". Here is the overall syntax as follows:

```
norm_image = cv2.normalize(closing, None, alpha = 0, beta = 1,
norm_type = cv2.NORM_MINMAX, dtype = cv2.CV_32F)
output2=norm_image.astype(np.uint8)
```
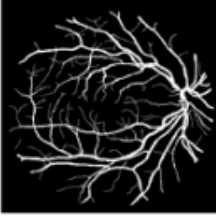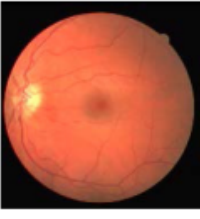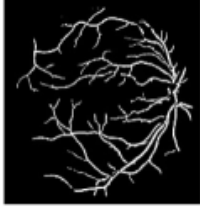
Table 1.   Segmentation result from DRIVE dataset.[25]
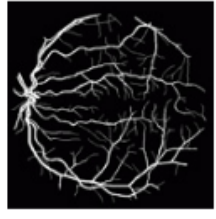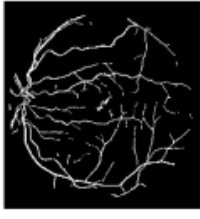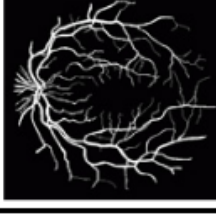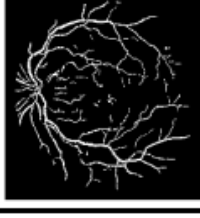
No.	Original Image	Ground Truth Image	Segmentation Image
1			
2			
3			
4			

Table 2.   Segmentation result from STARE dataset.[26]
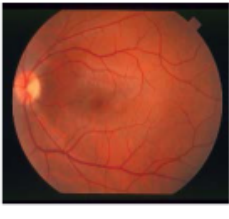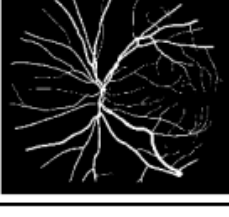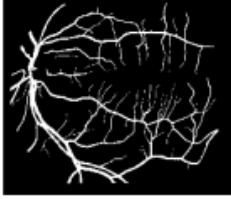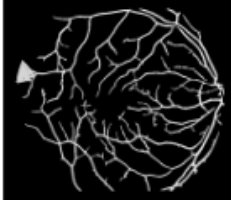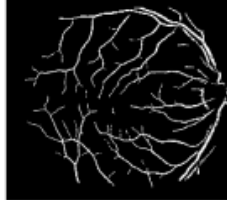
No.	Original image	Ground truth image	Segmentation image
1			
2			

Table 2. *(Continued)*

No.	Original image	Ground truth image	Segmentation image
3			
4			

```
output3 = cv2.normalize(output2, None, alpha = 0, beta = 255,
norm_type =cv2.NORM_MINMAX, dtype = cv2.CV_32F)
cv2.imwrite('F:/Newfolder/datatesting\Pyth/im0163.png',
closing)
cv2.imshow('results',closing)
cv2.waitKey(0) cv2.destroyAllWindows()
```

4. Discussion

It is important to measure research performance parameters. This illustrates how well the investigation was carried out using the retinal ground-truth dataset. The confusion matrix is a parameter method used to measure the compatibility of predictive data with ground truth data. The measurement parameters are Accuracy, Sensitivity, Specificity, Precision, and F1-Measure.

Accuracy scores are measurements that represent the proper correspondence of dataset outcomes and structures. The equation for Accuracy score can be seen in Eq. (8). Sensitivity or recall can be described as the proportion of nuclei of the retinal nutrition vessel to the number of nuclei of the blood vessels.[28] The equation for Sensitivity or recall score can be seen in Eq. (9). The specificity score defines the quantity of favorable class information given properly by the information collection placed on favorable information pairs, separated by the complete information.[28] The equation for the Specificity score can be seen in Eq. (10). Precision is an adequately categorized amount of beneficial samples separated by the complete sample as favorable.[29] The equation for the Precision score can be seen in Eq. (11). The F1 score or F1 metric is the median harmonic precision and recall, where the F1 score is highest at 1 (ideal accuracy and recall) and worst at 0. Properly F1 score is the best value and is suitable in evaluating the comparison of image

processing with ground truth dataset. The equation for the F1 Measure score can be seen in Eq. (12).

$$\text{Accuracy(Acc)} = \frac{\text{TP} + \text{TN}}{\text{TP} + \text{FN} + \text{TN} + \text{FP}}, \tag{8}$$

$$\text{Sensitivity or Recall(Se)} = \frac{\text{TP}}{\text{TP} + \text{FN}}, \tag{9}$$

$$\text{Specificity(Sp)} = \frac{\text{TN}}{\text{TN} + \text{FP}}, \tag{10}$$

$$\text{Precision(Prec)} = \frac{\text{TP}}{\text{TP} + \text{FN}}, \tag{11}$$

$$F1 \text{ Measure} = 2.\frac{\text{Precision} * \text{Recall}}{\text{Precision} + \text{Recall}}, \tag{12}$$

where

– TP stands for true positive, the quantity of favorable information that is properly represented by the scheme depending on the dataset.
– TN stands for true negative, which represents the amount of positive information displayed properly by the scheme depending on the information set.
– FN stands for false negative, the quantity of positive information but is balanced by the incorrect scheme dataset.
– FP stands for false positive, which is the amount of positive data but is matched based on the wrong dataset by the system.

Based on the equation for Accuracy (Acc) in Eq. (8), the equation for Sensitivity (Se) in Eq. (9), the equation for Specificity (Sp) in Eq. (10), the equation for Precision (Prec) in Eq.(11), and the equation for F1 Measure in Eq. (12), the results are obtained with the parameter measure execution time to DRIVE and STARE in Tables 3 and 4.

In image processing, the impact of the parameter values when viewed derives from the input values at a stage such as gamma values in the gamma correction stage, CLAHE parameter values, the constant value in image enhancement filter for sharpen filter and average filter, matrix kernel in sharpen filter and average filter, Sauvola threshold, median filters, and minimum size when small pixes have been removed. The parameter value for the measurement of the smaller and medium filters is very influential. It is very important to the importance of measuring parameters for removing the tiny pixels and the median filter.

The impact of the measuring parameter scores comes from two parts of the assessment parameters, namely, recall and precision, and the more significant the second element of the rating is, the more the valuation of the F1 score is and the easier the image processing is.

The measurement in Table 3 F1 measure for DRIVE shows that the file name 01 test.tif is the highest measuring value for F1, and in the file name, 08 test.tif, it is the

Table 3.   Results of measured parameters and execution time from DRIVE dataset.

File name (.tif)	Measurement parameters					Exe. time (s)
	Acc	Se	Sp	Prec	F1	
01_test	95.52	66.49	98.36	79.98	72.61	1.37
02_test	95.26	60.61	99.22	89.87	72.4	1.34
03_test	94.5	57.5	98.6	81.99	67.6	2.18
04_test	95.41	59.06	99.09	86.88	70.32	1.81
05_test	95.08	54.49	99.27	88.65	67.49	1.65
06_test	94.77	53.7	99.2	87.94	66.68	1.62
07_test	95.24	54.69	99.32	89.1	67.78	1.85
08_test	94.74	47.22	99.22	85.1	60.74	1.75
09_test	95.41	49.64	99.45	88.87	63.7	2.09
10_test	95.67	58.08	99.04	84.46	68.83	1.80
11_test	95.22	57.55	98.92	84.06	68.33	1.53
12_test	95.3	58.35	98.79	82.02	68.19	1.65
13_test	94.76	54.63	99.11	86.94	67.1	1.90
14_test	95.72	64.62	98.46	78.72	70.98	1.88
15_test	96.31	64.79	98.74	79.71	71.55	1.79
16_test	95.38	60.01	98.89	84.35	70.13	1.86
17_test	95.18	53.65	99.01	83.35	65.28	1.70
18_test	95.74	60.98	98.73	80.53	69.41	2.05
19_test	96.39	69.78	98.8	84.08	76.27	1.74
20_test	95.78	59.49	98.66	77.89	67.46	1.77
Avg	**95.37**	**58.27**	**98.94**	**84.22**	**68.64**	**1.77**

Table 4.   Results of measured parameters and execution time from STARE dataset.

File name (.ppm)	Measurement parameters					Exe. time (s)
	Acc	Se	Sp	Prec	F1	
im0001	93.88	40.78	98.48	70.05	51.55	2.04
im0002	95.01	39.53	98.97	73.31	51.37	1.90
im0003	95.27	62.67	97.35	60.09	61.35	1.32
im0004	93.61	14.67	99.93	94.52	25.39	1.83
im0005	94.29	63.46	97.36	70.49	66.79	1.40
im0044	95.37	66.27	97.55	66.98	66.62	2.23
im0077	95.38	68.64	97.71	72.39	70.47	1.65
im0081	95.65	61.94	98.37	75.47	68.04	1.41
im0082	95.58	63.36	98.34	76.52	69.32	2.04
im0139	94.24	65.49	96.75	63.84	64.66	2.56
im0162	96.24	70.7	98.2	75.13	72.85	2.31
im0163	96.44	74.18	98.31	78.76	76.35	1.92
im0235	95.42	62.05	98.68	82.14	70.7	2.57
im0236	95.31	60.59	98.77	83.09	70.08	2.54
im0239	94.45	47.97	98.84	79.67	59.89	2.07
im0240	93.81	45.32	99.33	88.56	59.95	2.95
im0255	95.89	68.85	98.55	82.4	75.02	2.41
im0291	96.54	40.5	99.53	82.19	54.27	1.99
im0319	96.45	23.78	99.72	79.7	36.63	1.98
im0324	94.55	21.15	99.8	88.47	34.14	1.91
Avg	**95.17**	**53.10**	**98.53**	**77.19**	**60.27**	**2.05**

lowest measurement for F1. The highest value of the F1 measurement can be found in the im0255.ppm file name while the lowest F1 measurement has a file name in the0004.ppm file. The DRIVE value is 68.64 when shown from the average value of F1, which is better than STARE 60.27. The accuracy of 95.37%, sensitivity of 58.27%, and 98.94% are measured according to Table 3 for the measurement value achieved for DRIVE.

The accuracy of 95.17%, sensitivity of 53.10%, and 98.53% are measured according to Table 4 for the measurement value achieved for STARE, which means that in this case, the values of the measurement parameters can be compared with previous studies as can be seen in Table 5.

The parameter value comparison with previous methods is based upon Tables 5 and 6, for DRIVE and STARE datasets that both precision and specificity parameters are better than previous method values in the proposed method. Still, the sensitivity value is less than the previous methods. In this research on the STARE, dataset image has a difficult challenge in getting binary retinal blood vessels because the image in the STARE dataset has many pixels that are homogeneous with the pixels of the retinal arteries and the range of pixels that are much the same between the pixels of the retinal vessels with non-pixel retinal blood vessels. However, the method proposed in this paper obtained significant results as evidenced in Tables 5 and 6.

The implementation time for each file is used to compare implementation time and device system requirements used in previous methods, with an average of 1.77 s for the DRIVE and 2.05 s for STARE. Due to the time execution in Tables 3 and 4,

Table 5. Results of DRIVE datasets segmentation in comparison to previous methods.

Method	Enhancement technique	Acc	Se	Sp
Pratap et al.[2]	Gauss Filter	93.74 %	—	—
Pal et al.[4]	CLAHE	92%	64%	95%
Kushol et al[30]	Top-hat and Bottom-hat	93.77%	62.96%	98.30%
Ray et al.[31]	Top-hat and Median Filter	94.02%	77.08%	99.01%
Khomri et al[12]	Top-hat Filter	94.5%	73.9%	97.4%
Proposed Method		95.37%	58.27%	98.94%

Table 6. Results of STARE datasets segmentation in comparison to previous methods.

Method	Enhancement technique	Acc	Se	Sp
Pratap et al.[2]	Gauss Filter	89.31%	—	—
Pal et al.[4]	CLAHE	89%	76%	89%
Kushol et al.[30]		—	—	—
Ray et al.[31]		—	—	—
Khomri et al[12]	Top-hat Filter	94%	73.2%	96.2%
Proposed Method		95.17%	53.10%	98.53%

Table 7. Comparison of DRIVE dataset with prior systems execution time and system demands.

Method	Execution Time	System Requirements
Pratap *et al.*[2]	2.61 s	1.65 GHZ. 2 GB RAM
Pal *et al.*[4]	—	—
Kushol *et al.*[30]	2–3 s	1.8 GHZ. 3 GB RAM
Ray *et al.*[31]	1.3 s	3.7 GHZ. 8 GB RAM
Khomri *et al.*[12]	2.21 s	2.6 GHZ. 4 GB RAM
Proposed Method	**1.77 s**	**1.4 GHZ. 2 GB RAM**

Table 8. Comparison of STARE dataset with prior systems execution time and system demands.

Method	Execution Time	System requirements
Pratap *et al.*[2]	2.40 s	1.65 GHZ. 2 GB RAM
Pal *et al.*[4]	—	—
Kushol *et al.*[30]	2.3 s	1.8 GHZ. 3 GB RAM
Ray *et al.*[31]	—	3.7 GHZ. 8 GB RAM
Khomri *et al.*[12]	3.14 s	2.6 GHZ. 4 GB RAM
Proposed Method	**2.05 s**	**1.4 GHZ. 2 GB RAM**

the structure of the pixels on the retinal image will affect the calculation of the execution time. Not only the structure of the pixels on the file type but also the size of the retinal image dimensions will affect the calculation of the execution time.

The comparison of execution time and device system requirements from the previous methods are presented in Tables 7 and 8. The methods used by the previous researchers[2,4,12,30,31] used devices with higher specifications for both frequency speed and RAM than the devices used in this study but resulted in faster time execution than previous studies. A similar analogy for experiments using the same specs would result in much faster execution times as a result of using higher spec than current devices.

Based on Table 7 when the approach is being run, the DRIVE dataset in the DRIVE section is of little value compared to the previous method, the Celeron processor 2957U 1,4 GHz Dual center portfolio has to low the system requirements device, and the Intel HD graphics, with 2 GB of RAM, also has sufficient time for STARE compared with the previous method. Hence, there is a smaller time[28] but used system requirements device core i3 6th gen CPU 3.7 GHz device, 8 GB of RAM.

5. Conclusion

The extraction of retinal images to acquire the blood vessels generated in this paper is quite a nice beginning point for pre-processes to obtain the output precision with image upgrade, processing, discoloration, etc. For data that regulate vessel extraction from the DRIVE and STARE datasets with precision, sensitivity, and specificity

parameters, retinal image processing experiments are available. Therefore, the proposed method for achieving average measurement values from the DRIVE dataset is 95.37% accuracy, 58.27% sensitivity, and 98.94% specificity. While 95.17% of the STARE dataset is accurate, it has 53.10% sensitivity and 98.53% specificity.

Compare the parameter numbers with the earlier technique in the suggested technique to make the price greater than the earlier technique for the DRIVES dataset, both precision and specificity parameters and impact scores are still smaller than those of the earlier technique, while the STARE dataset still has reduced scores than the earlier technique for precision, sensitivity, and specificities measuring parameters. In the image processing, the entry attributes at the point, such as gamma numbers at a gamma correction point, CLAHE parameter numbers, Sauvola threshold numbers, median filters, or min size, are applied to the extraction of tiny pixels.

The importance of the measuring parameter is very important for removing the tiny image and medium filter. This technique, however, is still not consistent with the outcomes of the treatment with essential facts or triggers, such as noise and root triggers of failure or blood vessel boost.

Acknowledgments

References

1. N. P. Singh and R. Srivastava, "Extraction of retinal blood vessels by using an extended matched filter based on second derivative of Gaussian," *Proceedings of the National Academy of Sciences India Section A Physical Sciences* **89**, 269–277 (2019).
2. M. Han, Y. Kim, J. R. Park, B. J. Vakoc, W. Y. Oh, and S. Ryu, "Retinal blood vessel caliber estimation for optical coherence tomography angiography images based on 3D superellipsoid modeling," *International Journal of Image and Graphics* **19**(02), 1950011 (2019).
3. A. Biran, P. S. Bidari, A. Almazroa, V. Lakshminarayanan and K. Raahemifar, "Blood vessels extraction from retinal images using combined 2D Gabor wavelet transform with local entropy thresholding and alternative sequential filter," *Canadian Conference on Electrical and Computer Engineering.* (2016), pp. 1–5.
4. A. L. Pal, S. Prabhu and N. Sampathila, "Extraction of retinal blood vessels from retinal fundus image for computer aided diagnosis," *Canar. E.college* (2015), pp. 400–403.
5. Z. Yavuz and C. Köse, "Blood vessel extraction in color retinal fundus images with enhancement filtering and unsupervised classification," *Journal of Healthcare Engineering* **2**, 1–12 (2017).

6. J. Dash, "Retinal blood vessels extraction from fundus images using an automated method," *2018 4th International Conference on Recent Advances in Information Technology (RAIT)* (2018), pp. 1–5.

7. J. Dash and N. Bhoi, "An unsupervised approach for extraction of blood vessels from fundus images," *Journal of Digital Imaging* **31**(10), 857–868 (2018).

8. D. Güu, "A novel retinal vessel extraction method based on dynamic scales allocation," *International Conference on Image and Vision Computing* (2017), pp. 145–149.

9. T. A. Soomro, "Retinal blood vessel extraction method based on basic filtering schemes," *IEEE International Conference on Image Processing (ICIP)* (2018), pp. 4422–4426.

10. M. Ben Abdallah *et al.*, "Automatic extraction of blood vessels in the retinal vascular tree using multiscale medialness," *International Journal of Biomedical Imaging* **2015**, 1–16 (2015).

11. R. Kamble, "Automatic blood vessel extraction technique using phase stretch transform in retinal images, *2016 International Conference on Signal and Information Processing (IConSIP)* (2017), pp. 1–5.

12. B. Khomri, A. Christodoulidis, L. Djerou and M. C. Babahenini, "Retinal blood vessel segmentation using the elite-guided multi-objective artificial bee colony algorithm," *IET Image Processing* **12**, 2163–2171 (2018).

13. Erwin and T. Yuningsih, "Detection of blood vessels in optic disc with maximum principal curvature and wolf thresholding algorithms for vessel segmentation and Prewitt edge detection and circular hough transform for optic disc detection," *Iranian Journal of Science and Technology Transactions of Electrical Engineering* **45**(2), 1–12 (2020).

14. Erwin and D. R. Ningsih, "Improving retinal image quality using the contrast stretching, histogram equalization, and CLAHE methods with median filters," *International Journal of Image, Graphics and Signal Processing* **12**(2), 30–41 (2020).

15. Erwin, A. Noorfizir, M. N. Rachmatullah, Saparudin and G. Sulong, "Hybrid multilevel thresholding-otsu and morphology operation for retinal blood vessel segmentation," *Engineering Letters* **28**(1), 180–191 (2020).

16. Erwin and T. Kiyatmoko, "Retinal vessel extraction using dynamic threshold and enhancement image filter from retina fundus," *Journal of Information Systems and Telecommunication* **6**(24), 189–196 (2019).

17. Erwin, M. N. Rachmatullah and W. Saputri, "Automatic detection of background diabetic retinopathy disease using hybrid multilevel thresholding and convolutional neural network," *Journal of Engineering Science and Technology* **14**(5), 2522–2539 (2019).

18. S. K. Panigrahi and S. Gupta, "Joint bilateral filter for signal recovery from phase preserved curvelet coefficients for image denoising," *International Journal of Image and Graphics* **21**(4), 2150049 (2021).

19. H. Salehi and J. Vahidi, "A novel hybrid filter for image despeckling based on improved adaptive wiener filter, bilateral filter and wavelet filter," *International Journal of Image and Graphics* **21**(03) 2150036 (2021).

20. S. A. Amiri, "A preprocessing approach for image analysis using gamma correction," *International Journal of Computer Applications* **38**(12), 38–46 (2012).

21. A. L. I. M. Reza, "Realization of the contrast limited adaptive histogram equalization (CLAHE) for real-time image enhancement," *Journal of VLSI Signal Processing* **38**, 35–44 (2004).

22. J. Sauvola and M. Pietika, "Adaptive document image binarization," *Pattern Recognition* **33**, 225–236 (2000).

23. N. Mahua and M. Banerjee, "A comparative analysis of application of Niblack and Sauvola binarization to retinal vessel segmentation," *2017 International Conference on Computational Intelligence and Networks* (2017), pp. 105–109.

24. R. C. Gonzalez and R. E. Woods, *Digital Image Processing*, 3rd edn. (Prentice-Hall, Inc. Upper Saddle River, NJ, USA, 2007).
25. J. J. Staal, M. D. Abramoff, M. Niemeijer, M. A. Viergever and B. van Ginneken, "Ridge based vessel segmentation in color images of the retina," *IEEE Transactions on Medical Imaging* **23**(4), 501–509 (2004).
26. A. Hoover, "Locating blood vessels in retinal images by piecewise threshold probing of a matched filter response," *IEEE Transactions on Medical Imaging* **19**(3), 203–210 (2000).
27. A. Hoover and M. Goldbaum, "Locating the optic nerve in a retinal image using the fuzzy convergence of the blood vessels," *IEEE Transactions on Medical Imaging* **22**(8), 951–958 (2003).
28. H. B. Wong and G. H. Lim, "Measures of diagnostic accuracy: Sensitivity, specificity, PPU and NPV," in *Proc. Singapore Healthcare* (2011), pp. 316–318.
29. C. Goutte and E. Gaussier, "A probabilistic interpretation of precision, recall and F-score, with implication for evaluation," in *Proc. European Colloquium on IR Resarch (ECIR'05)* (2005), pp. 345–359.
30. R. Kushol, M. H. Kabir, M. S. Salekin and A. B. M. A, Rahman, "Contrast enhancement by top-hat and bottom-hat transform with optimal structuring element: Application to retinal vessel segmentation," Springer International Publishing AG 2017, pp. 533–540.
31. A. Ray, A. Chakraborty, D. Roy, B. Sengupta and M. Biswas, "Blood vessel extraction from fundus image," *Emerging Technologies in Data Mining and Information Security* (2018), pp. 259–268.

Erwin was born in Palembang, Indonesia, in 1971. He is a Lecturer at the Department of Computer System, Faculty of Computer Science, Sriwijaya University, Indonesia. He received his Bachelor degree in Mathematics from the University of Sriwijaya, Indonesia, in 1994 and his M.Sc. degree in Acturial from the Bandung Institute of Technology (ITB), Bandung, Indonesia, in 2002. He received his Doctorate in Engineering from Faculty of Engineering, Sriwijaya University, Indonesia, in 2019. His current research interests include image processing and computer vision. Erwin is a member of IAENG and IEE. He is the chairperson of the Sriwijaya Image Digital and Forensic (SIDaF) Research Group at the University of Sriwijaya, Indonesia.

Hadrians Kesuma Putra was born in Baturaja, Indonesia, in 1977. He received his medical degree of Medical Faculty from Sriwijaya University, Indonesia, in 2002, and an ob-gyn specialist degree in Medical Faculty from Sriwijaya University, Indonesia, in 2009. In 2005, he joined Sriwijaya University as a Lecturer.

Bambang Suprihatin was born in Salatiga, Indonesia, in 1971. He received his Bachelor of Mathematics from Sriwijaya University, Indonesia, in 1994, and an M.Sc. degree in Mathematics from the Bandung Institute of Technology (ITB), Bandung, Indonesia, in 2002. In 1994, he joined Sriwijaya University as a Lecturer. He was an Associate Professor in 2011. He received his Doctorate in Mathematics, Universitas Gadjah Mada (UGM) in 2016. His current research interests are statistics and modeling.

Fathoni was born in Palembang, Indonesia, in 1972. In 2020. He is currently working on a project for his Doctorate in Engineering, Faculty of Engineering, Sriwijaya University, Indonesia. He received his bachelors' degree in informatics management and computer engineering from the Institut Sains dan Teknologi Akprind in 1998 and magister of information system from Universitas Gunadarma in 2001. In 2008, he joined as a lecturer at Information System Department in Universitas Sriwijaya where is working until now. His current research interests include the field of data mining, pattern recognition, and artificial intelligence.

Retinal Blood Vessel Extraction Using a New Enhancement

18%	**14**%	**10**%	**5**%
SIMILARITY INDEX	INTERNET SOURCES	PUBLICATIONS	STUDENT PAPERS

MATCH ALL SOURCES (ONLY SELECTED SOURCE PRINTED)

3%

★ Submitted to Sriwijaya University

Student Paper

Exclude quotes	On		Exclude matches	Off
Exclude bibliography	On			